Numerical Simulation of Natural Convection of Glycol-Al_2O_3 Nanofluids from a Horizontal Cylinder

Dorota Sawicka[a,b], Albert Baars[a], Janusz T. Cieśliński[b], Sławomir Smoleń[a]

[a)] City University of Applied Sciences Bremen, Neustadtswall 30, 28199 Bremen, Germany
[b)] Gdańsk University of Technology, Faculty of Mechanical Engineering, ul. Narutowicza 11/12, 80-233 Gdańsk, Poland

Address correspondence to Dorota Sawicka, City University of Applied Sciences Bremen, Neustadtswall 30, 28199 Bremen, Germany. E-mail: sawicka.dorota@hotmail.com
Phone Number: +49 1573 1915195, Fax Number: +49 421 5905 3575

ABSTRACT

This paper deals with natural convection around a circular cylinder with constant heat flux in a cavity using computation fluid dynamics. As fluids ethylene glycol and a mixture of ethylene glycol with Al_2O_3 nanoparticles (mass concentrations of nanoparticles: 0.1% and 1%) are chosen. Rayleigh number ranges from $3 \cdot 10^4$ to $3 \cdot 10^5$. The nanofluids are modeled with single-phase approach. For the investigated range of nanoparticle concentration, the influence of concentration on Nusselt, Rayleigh number and heat transfer coefficient is small. Nevertheless, a slight shift towards lower Nusselt, Rayleigh numbers and an increase in heat transfer coefficient occur. The Nusselt number depends on Rayleigh number and only negligible on Prandtl number, which is in accordance with literature for Prandtl numbers of around 200. The numerically obtained results are compared with own preliminary experimental data, deviations are discussed.

INTRODUCTION

Nanofluids are two-phase mixtures of conventional fluids used in heat exchangers and solid particles of sizes below 100 nm (Choi and Eastman [1]). The fact that thermal conductivity of these suspensions is higher than that of the base liquids results from the higher thermal conductivities of solids in comparison to liquids [2, 3]. Nanofluids came to be seen as a new generation of coolants in single and two phase systems. Furthermore, nanofluids or nanocomposites may be used as media in thermal energy storages, as sensible heat storage and phase change materials. In the SHS systems the dominating heat transfer mechanism is natural convection. However, in literature only a few investigations of free convection of nanofluids have been published. Moreover, these results of numerical and experimental investigations of free convection of nanofluids often seem to be contradictory. Minea and Lorenzini [4] study numerically natural convective heat transfer of ZnO-water nanofluids in a rectangular enclosure for a constant heat flux and nanoparticle volume fractions ranging from 1% to 4% and Rayleigh numbers of 10^4 to 10^6. The results show that addition of nanoparticles to base fluid cause a low change in Nu number (Nu_{nf}/Nu_{bf} =0.95 to 1.01 for a nanoparticle volume fraction of 1%, depending on Rayleigh number and location of the heated surface). Yu et al. [5] investigate numerically transient natural convection heat transfer of CuO-water nanofluids in a horizontal annulus between two coaxial cylinders with constant temperature boundary conditions, constant Prandtl number Pr = 7 and Rayleigh numbers of 10^4 and 10^5. The volume fraction of nanoparticles ranges from 0 to 0.05. This work shows, that while the nanoparticle volume fraction increases the time averaged Nusselt number is lowered by up to 10% while the temporal flow development is almost independent of the volume fraction of nanoparticles. Oztop and Abu-Nada [6] investigate numerically natural convective heat transfer of different types of water-based nanofluids in a partially heated enclosure with constant temperature

boundary conditions. For Rayleigh numbers of 10^3 to $5 \cdot 10^5$ an increase of Nusselt number with growing volume fraction of nanoparticles is found. They note the highest increase in Nu of 40% at a nanoparticle volume fraction of 0.2. Guestal et al. [7] investigate numerically natural convection of Cu-water and TiO_2-water nanofluids in a partially heated horizontal cylindrical enclosure with constant temperature boundary conditions. The study shows that the Nusselt number rises linearly with increasing volume fraction of nanoparticles. The maximum change of Nusselt number of 15.7% appears for the Cu-water nanofluid with a volume fraction of 0.05.

This work aims to evaluate the potential of ethylene glycol-Al_2O_3 nanofluids as a sensible heat storage material in a natural convection system using computational fluid dynamics. The tested rectangular geometry simulates a SHS container. A horizontal cylinder with a constant heat flux boundary condition serves as heating element. Al_2O_3 nanoparticles are considered with weight fractions of 0.1% and 1%. The results of numerical simulations are presented and compared to own preliminary experimental data, received with similar boundary conditions. The Rayleigh number ranges from $3 \cdot 10^4$ to $3 \cdot 10^5$ comparable with own experimental investigations.

MATERIALS AND METHODS

The numerical study in this work is based on an experimental set up. In the latter the test chamber is of cuboid shape made of acrylic glass with inside dimensions of 160 mm x 160 mm x 500 mm, filled with fluid to a level of 380 mm. A commercially available stainless steel tube of 10 mm outer diameter, 0.6 mm wall thickness and 150 mm effective length is used as resistance heater. The results of the experimental investigations serve to evaluate those of the numerical simulations. The computational space is two-dimensional with the dimensions of 160 mm x 380 mm (Figure 1). The heating section consists of a horizontal cylinder with a diameter of 10 mm. For the tested Rayleigh number range of $3 \cdot 10^4$ to $3 \cdot 10^5$ a constant heat flux (5002, 10005 and 15007 W/m^2) is

applied. The walls are considered to be adiabatic and have no-slip boundary condition (Figure 1). The single phase approach is used for this study. The thermophysical properties of the nanofluids are considered to be constant in time and space.

Governing equations and numerical method

Continuity, momentum and energy equation for a Newtonian fluid, constant fluid properties and with Boussinesq approximation

$$\frac{\partial u_i}{\partial x_i} = 0 \tag{1}$$

$$\rho \frac{Du_i}{Dt} = -\frac{\partial p}{\partial x_i} + \mu \frac{\partial^2 u_i}{\partial {x_j}^2} + \rho(1 - \beta(T - T_c))g_i \tag{2}$$

$$\rho c_p \frac{DT}{Dt} = k \frac{\partial^2 T}{\partial {x_i}^2} \tag{3}$$

are solved by the finite volume open source code OpenFOAM 4.1 (Open source Field Operation and Manipulation) [8]. The discretization of the equations is of second order in time and first order in space. The maximum Courant number amounts to 0.8.

During the simulation the temperature of the fluid is registered in 6 points and the temperature of the cylinder's wall in 4 points.

The temperature probes have the following coordinates in millimetres:

$t_{f1} = (-30\ 100\ 0)$, $t_{f2} = (30\ 100\ 0)$

$t_{f3} = (-30\ 50\ 0)$, $t_{f4} = (30\ 50\ 0)$

$t_{f5} = (-30\ 0\ 0)$, $t_{f6} = (30\ 0\ 0)$

$t_{w1} = (0\ 5\ 0)$, $t_{w2} = (5\ 0\ \ 0)$

$t_{w3} = (0\ -5\ 0)$, $t_{w4} = (-5\ 0\ \ 0)$

The hybrid grid is generated with GMSH 2.10.1 [9] mesh generator and consists of 63054 cells (Figure 2). A grid study has been carried out.

Thermophysical properties of nanofluids

The following correlations are used to calculate the thermophysical properties of the investigated nanofluids.

To determine the density of water with suspended Al_2O_3 and TiO_2 nanoparticles at a temperature of 25°C and volume concentrations up to 4.5% Pak and Cho [10] used the equation

$$\rho_{nf} = \varphi_v \rho_p + (1 - \varphi_v)\rho_{bf} \tag{4}$$

Here, φ_v denotes the volume fraction of nanoparticles, $\rho_p$the density of nanoparticles and ρ_{bf} the density of the base fluid. For determination of the kinematic viscosity of nanofluids the Einstein model [11] is used

$$\mu_{nf} = \mu_{bf}(1 + 2.5 \cdot \phi_v) \tag{5}$$

This model is suitable for low fractions and a spherical form of nanoparticles. The thermal conductivity is calculated with the Maxwell model [12]

$$k_{nf} = \frac{2k_{bf} + k_p + 2\varphi_v(k_p - k_{bf})}{2k_{bf} + k_p - \varphi_v(k_p - k_{bf})} \cdot k_{bf} \tag{6}$$

The specific heat capacity is calculated with a relation by Pak and Cho [10]

$$c_{p(nf)} = \varphi_v c_{p(p)} + (1 - \varphi_v)c_{p(bf)} \tag{7}$$

This model is based on the volume concentration of nanoparticles and is taking the idea from the liquid- particle mixture formula. The thermal expansion coefficient is determined from

$$\beta_{nf} = \frac{(1-\varphi_v)\beta_{bf}\rho_{bf} + \varphi_v \rho_p \beta_p}{\rho_{nf}} \tag{8}$$

This equation considers densities and thermal expansion coefficients of nanoparticles and base fluid used in various studies [13-17]. Thermophysical properties of ethylene glycol and applied Al_2O_3 nanoparticles are presented in the Table 1 [18, 19].

Data analysis

The average heat transfer coefficient is calculated by

$$\alpha = \frac{\dot{q}}{\Delta T} \tag{9}$$

with the temperature difference

$$\Delta T = T_w - T_f \tag{10}$$

The wall temperature T_w is determined as an average of the temperature probes on the cylinder surface registered during the simulation

$$T_w = \frac{1}{4}\sum_{k=1}^{4} T_{wk} \tag{11}$$

The fluid temperature is also calculated as an average from the probes located at diverse positions in the computational domain

$$T_f = \frac{1}{6}\sum_{k=1}^{6} T_{fk} \tag{12}$$

Nusselt and Rayleigh numbers are received from

$$Nu = \frac{\alpha d}{k} \tag{13}$$

$$Ra = \frac{g\beta\Delta T d^3}{\nu a} \tag{14}$$

The characteristic length is the diameter *d* of the cylinder. The numerical results are compared with the correlation by Churchill and Chu [20] for natural convection heat transfer of a horizontal cylinder and conventional single-phase fluids.

$$Nu_{ch} = \left\{ 0.6 + \frac{0.387 \cdot Ra^{\frac{1}{6}}}{\left[1+\left(\frac{0.559}{Pr}\right)^{\frac{9}{16}}\right]^{\frac{8}{27}}} \right\}^2 \tag{15}$$

The correlation holds over the range of $0 < Pr < \infty$ and $10^{-5} \leq Ra \leq 10^{12}$.

RESULTS AND DISCUSSION

In Figure 3 velocity fields at three different times are shown for $\dot{q} = 10005\,\mathrm{W/m^2}$. For all three time steps two different spatial domains can be recognised: In the region above the cylinder fluid motion due to free convection appears, the region under the cylinder is characterised by much slower velocities. With time the behaviour of fluid motion changes and can be divided into three phases. Phase 1: From the beginning until 200 s, an almost symmetric velocity field develops. Driven by horizontal density gradients, a free jet moves in the centre of the cavity from the vicinity of the cylinder towards the upper boundary. There, the jet is deflected. Due to continuity reason two recirculation areas occur to the right and left of the jet. Phase 2: The jet gets unstable, undulates in lateral direction and finally attaches to one of the vertical walls, in this case to the right wall. This process ends at about 375 s. Above the cylinder one recirculation domain appears. Phase 3: The latter state gets also unstable and runs over to a highly transient one in which the jet partially detaches from the vertical walls. Within this process the locations of recirculation areas change with time.

Figure 4 presents the progressions of temperatures with time for different locations, in the fluid and on the cylinder wall. As expected the highest temperatures appear on the cylinder wall and the maximum at the highest position. This results from the constant heat flux boundary condition and that already heated fluid passes this point. Within the chosen locations temperature differences on the cylinder wall amount to ≈ 10 K and in the fluid to ≈ 1 K. The different phases mentioned before can be recognised in the progression of curves.

The numerical model is evaluated by the comparison of Nu versus Ra with own preliminary experimental results and the correlation of Churchill and Chu [20] (Figure 5). The presented Nusselt and Rayleigh numbers from the numerical simulation are calculated at the end of phase 2.

The results of the numerical simulation agree quite well with those from the correlation of Churchill and Chu. They show slightly higher values of Nusselt number. An explanation could be that the recirculation of the flow in the upper part of the cavity intensifies the heat transfer at the cylinder. Furthermore, the grid study shows that a higher spatial resolution of the grid leads to a reduction in deviation. The experiments deliver a similar progression of Nu versus Ra but higher values in comparison to data from Churchill and Chu [20] as well as from numerical simulation. An apparent difference between the data sets is, that the experiment is a three dimensional case while for the others a two dimensional flow is assumed. In addition, the experimental data are taken in phase 3 and not at the end of phase 2. According to Ra, calculated with the cylinder diameter, the undisturbed free convective flow in the vicinity of the cylinder can be considered as laminar. This may not be valid for the upper part of the cavity. Due to recirculation of the fluid turbulent flow may intensify the heat transfer process around the cylinder and lead to higher values of Nu. So far no turbulence model is used for the numerical simulation. To uncover this, further numerical and experimental studies are necessary. The influence of nanoparticle fraction on the progression of Nu versus Ra, received from numerical simulation, is small. The maximal decrease of Nu number amounts to around 1.5% for $Ra = 2 \cdot 10^5$ and both analysed nanoparticle concentrations (0.1%, 1%). For both concentrations a shift towards lower Ra and Nu numbers (Figures 5 and 6) appears but the data points almost remain on the curve of Churchill and Chu [20]. This seems to be reasonable: (a) The correlation of Churchill and Chu delivers that the influence of the Prandtl number on Nu for values of $Pr > 100$ is rather small, see Figure 7. (b) The Prandtl number of EG with and without nanoparticles is in the order of 200, see Figure 8. Therefore, Nu depends nearly solely on Ra and the data points for different nanoparticle concentration lay on one curve. An explanation for the downward shift of Nu and Ra with

nanoparticle concentration can be given as follows: As mentioned in the introduction a rise in heat conductivity with concentration occurs, see Figure 9. Since the heat flux at the cylinder wall can be expressed by the product of heat conductivity and negative surface normal temperature gradient, the latter decreases at constant heat flux and rising nanoparticle concentration. From this one can conclude that the temperature difference between cylinder surface and fluid decreases and that the heat transfer coefficient grows (Figure 9). The latter grows less strong in comparison to the heat conductivity (Figure 10), which leads to a decline in Nu number. At smaller temperature differences between cylinder wall and fluid, lower density gradients in the fluid and therefore less fluid motion due to free convection arise. In addition, an increase in viscosity with nanoparticle concentration occurs. This may explain why α rises less than k. For the investigated Prandtl number, a decline in Nu is linked with a decline in Ra.

The comparison of our results with those from literature is not obvious due to different geometries, boundary conditions and nanofluids. Minea and Lorenzini [4] found both, increase and decrease of Nu number with nanoparticle concentration. The absolute values of change (up to 3%) are in the range, found in our study. For heat transfer coefficient, they calculated an increase of around 2-4% for a volume concentration of 1% in the range of $Ra=10^4$ to $3\cdot10^5$. This fits to our results. In contrast this does not hold for the progression of heat transfer coefficient with/without nanoparticles over Ra. Yu et al. [5] noted also a decrease of Nu number with volume fraction of nanoparticles. A comparison with the results of this work is not apparent, because the Prandtl number is constant in their investigations.

Different behavior was reported by Oztop et al. [6] and Guestal et al. [7]. For all of the tested nanofluids and Ra number range, an increase of Nu number was noted with nanoparticle volume fraction.

The experimental data of Nu versus Ra for EG with and without nanoparticles are given in Figure 11. For constant Ra the data suggests a maximum of Nu at a concentration of 0.1%. Here, a maximal increase of 16% can be observed. The results of the numerical simulations do not reflect this behaviour. At this point one can speculate that the consideration of nanoparticles in the fluid by thermophysical properties is not sufficiently accurate. As noted by Yu et al. [5], a model without considering the Brownian motions of nanoparticles leads to an overestimation of Nu number. Hence, in the next steps the calculation of the thermophysical properties have to be revised as well as the experimental set-up of these preliminary results.

CONCLUSIONS

Free convective heat transfer of ethylene glycol with and without Al_2O_3 nanoparticles (0.1 and 1% by mass) around a cylinder located in a cavity is investigated using 2D computational fluid dynamics. On the cylinder wall a constant heat flux boundary condition is applied. Nanoparticles are only considered by thermophysical properties. The investigated range of Rayleigh number is $3 \cdot 10^4$ to $3 \cdot 10^5$. The results in form of Nusselt versus Rayleigh number are compared to an empirical correlation (Churchill and Chu [20]) and to own preliminary experimental data. As expected all these data sources show a nonlinear increase of Nu with Ra. Results from numerical simulation agree quite well with those of the correlation by Churchill and Chu [20]. The increase in nanoparticle concentration leads to a decrease in Nu, Ra number and an increase in heat transfer coefficient. The latter findings indicate, that the tested nanofluid could be suitable for use in a sensible storage. The calculated data for Nu versus Ra lay on one curve. The reason are Prandtl numbers of the fluids of around 200, where the relation of Nu versus Ra is nearly independent on Pr. The shift of Nu and Ra with nanoparticle concentration can be explained by change of thermophysical properties. The experimental results feature higher values of Nu at equal Ra

numbers in comparison to those of the empirical correlation and of the numerical simulation. Furthermore, the data points for different nanoparticles concentrations do not lay on one curve. Reasons may be two-dimensional simulations or the simple model to consider nanoparticles. Here, further investigations are necessary.

NOMENCLATURE

a	thermal diffusivity, m^2/s
Al_2O_3	aluminum oxide
c_p	specific heat capacity, J/(kg K)
d	outer diameter of heated cylinder, m
EG	ethylene glycol
g	gravitational acceleration, m/s^2
k	thermal conductivity, W/(m K)
n	surface normal coordinate, m
Nu	Nusselt number
p	pressure, Pa
Pr	Prandtl number
$\acute{q}$	heat flux, W/m^2
Ra	Rayleigh number
SHS	sensible heat storage
t	time, s
T	temperature, K
ΔT	temperature difference, K
u	velocity, m/s

x coordinate, m

Greek symbols

α heat transfer coefficient, W/(m^2 K)

β thermal expansion coefficient, 1/K

μ dynamic viscosity, Pa s

ν kinematic viscosity, m^2/s

φ nanoparticle concentration

ϕ nanoparticle fraction

ρ density, kg/m^3

Subscripts

bf base fluid

c reference

ch Churchill and Chu [20]

f fluid

i, j, k index notation

m mass

nf nanofluid

p particle

v volume

w wall

REFERENCES

[1] Choi S. US., Eastman JA., Enhancing thermal conductivity of fluids with nanoparticles, *Tech. rep. Argonne National Lab*., IL (United States), 1995.

[2] Cieśliński J.T., Krygier K., Smoleń S., Measurement of temperature-dependent viscosity and thermal conductivity of alumina and titania thermal oil nanofluids, *Archives of Thermodynamics*, vol. 36, No. 4, pp. 35-47, 2015.

[3] Cieśliński J.T., Krygier K., Smoleń S., Influence of nanoparticle concentration on thermal properties of thermal oil-MWCNT nanofluids, *Applied Mechanics and Materials*, vol. 831, pp. 198-207, April 2016

[4] Minea A.A., Lorenzini G., A numerical study on ZnO based nanofluids behavior on natural convection, *International Journal of Heat and Mass Transfer*, vol. 114, pp. 286-296, November 2017

[5] Yu Z.-T., Wang W., Xu X., Fan L.-W., Hu Y.-C., Cen K.-F., A numerical investigation of transient natural convection heat transfer of aqueous nanofluids in a horizontal concentric annulus, *International Journal of Heat and Mass Transfer*, vol. 55, No. 4, pp. 1141-1148, 2012

[6] Oztop H. F., Abu-Nada E., Numerical study of natural convection in partially heated rectangular enclosures filled with nanofluids, *International Journal of Heat and Fluid Flow*, vol. 29, No. 5, pp. 1326-1336, 2008

[7] Guestal M., Kadja M., Hoang M. T., Study of heat transfer by natural convection of nanofluids in a partially heated cylindrical, *Case Studies in Thermal Engineering*, vol. 11, pp. 135-144, March 2018

[8] OpenFOAM: https://openfoam.org/, 22.11.2018

[9] Geuzaine C., Remacle J.-F., Gmsh: a three-dimensional finite element mesh generator with built-in pre- and post-processing facilities, *International Journal for Numerical Methods in Engineering*, vol. 79, no.11, pp. 1309-1331, 2009.

[10] Pak BC., Cho YI., Hydrodynamic and heat transfer study of dispersedfluids with submicron metallic oxide particles. *Exp Heat Transf Int J*, vol.11, no.2, pp. 151–70, 1998

[11] Einstein A., A new determination of molecular dimensions. Ann Phys, vol. 19, no.2, pp. 289–306, 1906.

[12] Maxwell JC., A treatise on electricity and magnetism, *Clarendon press*, vol. 1, 1st ed., Oxford, 1873.

[13] Khanafer K., Vafai K., A critical synthesis of thermophysical characteristics of nanofluids, *Int. J. Heat Mass Transfer*, vol. 54, No. 19-20, pp. 4410–4428, 2011.

[14] Ho C.J., Liu W.K., Chang Y.S., Lin C.C., Natural convection heat transfer of aluminawater nanofluid in vertical square enclosures: an experimental study, *Int. J. Therm.Sci*., vol. 49, No. 8, pp. 1345–1353, 2010.

[15] Khanafer K., Vafai K., Lightstone M., Buoyancy-driven heat transfer enhancement in a two-dimensional enclosure utilizing nanofluids, *Int. J. Heat Mass Transfer*, vol.46, pp. 3639–3653, 2003.

[16] Khalili E., Saboonchi A., Saghafian M., Natural Convection of Al_2O_3 Nanofluid Between Two Horizontal Cylinders Inside a Circular Enclosure, *Heat Transfer Engineering*, vol.38, no.2, pp. 177-189, 2017

[17] Snoussi L., Ouerfelli N., Chesneau X., Chamkha A.J., Belgacem F.B.M, Guizani A., Natural Convection Heat Transfer in a Nanofluid Filled U-Shaped Enclosures: Numerical Investigations, *Heat Transfer Engineering*, vol. 39, no.16, pp. 1450-1460, 2018.

[18] Incropera F.P., De Witt D.P., Bergman T.L., Lavine A.S., *Fundaments of Heat and Mass Transfer*, 6th ed., John Wiley & Sons, New York, United States of America, 2007.

[19] Wefers K., Misra Ch., Oxides and Hydroxides of Aluminium, *ALCOA Laboratories Technical Paper, No.19*, Alcoa Laboratories, Freeport Road, New Kensington, Westmoreland County, PA, United States of America, 1987.

[20] Churchill S.W., Chu H.H.S., Correlating equations for laminar and turbulent free convection from a horizontal cylinder, *Int. J. Heat and Mass Transfer*, vol. 18, No. 9, pp. 1049-1053, 1975.

Table 1 Thermophysical properties of ethylene glycol and considered nanoparticles [18]

Property	Ethylene glycol	Al_2O_3-nanoparticles
Density, ρ in kg/m^3	1115.3	3970

Dynamic viscosity, μ in Pa s	0.022	-
Specific heat capacity,c_p in J/(kgK)	2391.9	795
Thermal conductivity, k in W/(mK)	0.2412	46
Prandtl number, Pr	214	-
Thermal expansion coefficient, β in 1/K	0.00065	$5.5 \cdot 10^{-6}$ [19]

List of Figure Captions

Figure 1 Scheme of the computational domain with boundary conditions and probes (f_1-f_6, w_1-w_4)

Figure 2 Mesh of the computational domain (left: whole computation space, right: detail of the mesh around the heated cylinder)

Figure 3 Velocity field (colour: magnitude of velocity, arrows: flow direction) for a heat flux $\dot{q} = 10005\,\mathrm{W/m^2}$

Figure 4 Temperature development with time at diverse locations of the calculation domain

($t_{f1} \div t_{f6}$ – temperatures in the fluid; $t_{w1} \div t_{w4}$ – temperatures on the cylinder wall)

Figure 5 Nusselt versus Rayleigh number from the numerical simulation for EG with and without nanoparticles in comparison to the correlation of Churchill and Chu [20] and preliminary experimental results

Figure 6 Nusselt number versus nanoparticle concentration for a heat flux of $\dot{q} = 10005\, W/m^2$

Figure 7 Nusselt versus Rayleigh number for different Prandtl numbers calculated from the correlation of Churchill and Chu [20]

Figure 8 Prandtl number versus concentration of nanoparticles for EG-Al_2O_3 nanofluid and a temperature of 295 K

Figure 9 Ratio of heat transfer coefficient with and without nanoparticles versus Rayleigh number for nanoparticle mass concentrations of 0.1% and 1%

Figure 10 Influence of nanoparticle concentration φ on mean temperature difference between cylinder wall and fluid ΔT as well as heat conductivity k for the heat flux $\dot{q} = 10005\ \mathrm{W/m^2}$. The plotted quantities for the nanofluid (nf) are related to those of ethylene glycol (bf)

Figure 11 Nusselt versus Rayleigh number for ethylene glycol-Al_2O_3 nanofluids with different nanoparticle mass concentrations from the experimental study

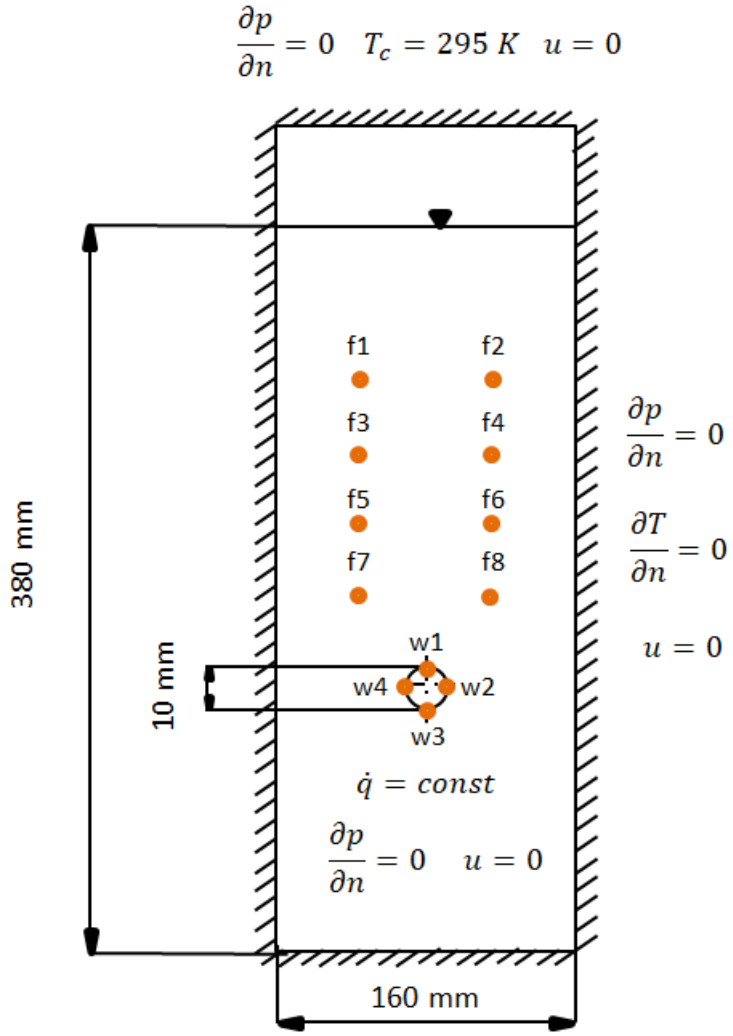

Figure 1 Scheme of the computational domain with boundary conditions and probes (f_1-f_6, w_1-w_4)

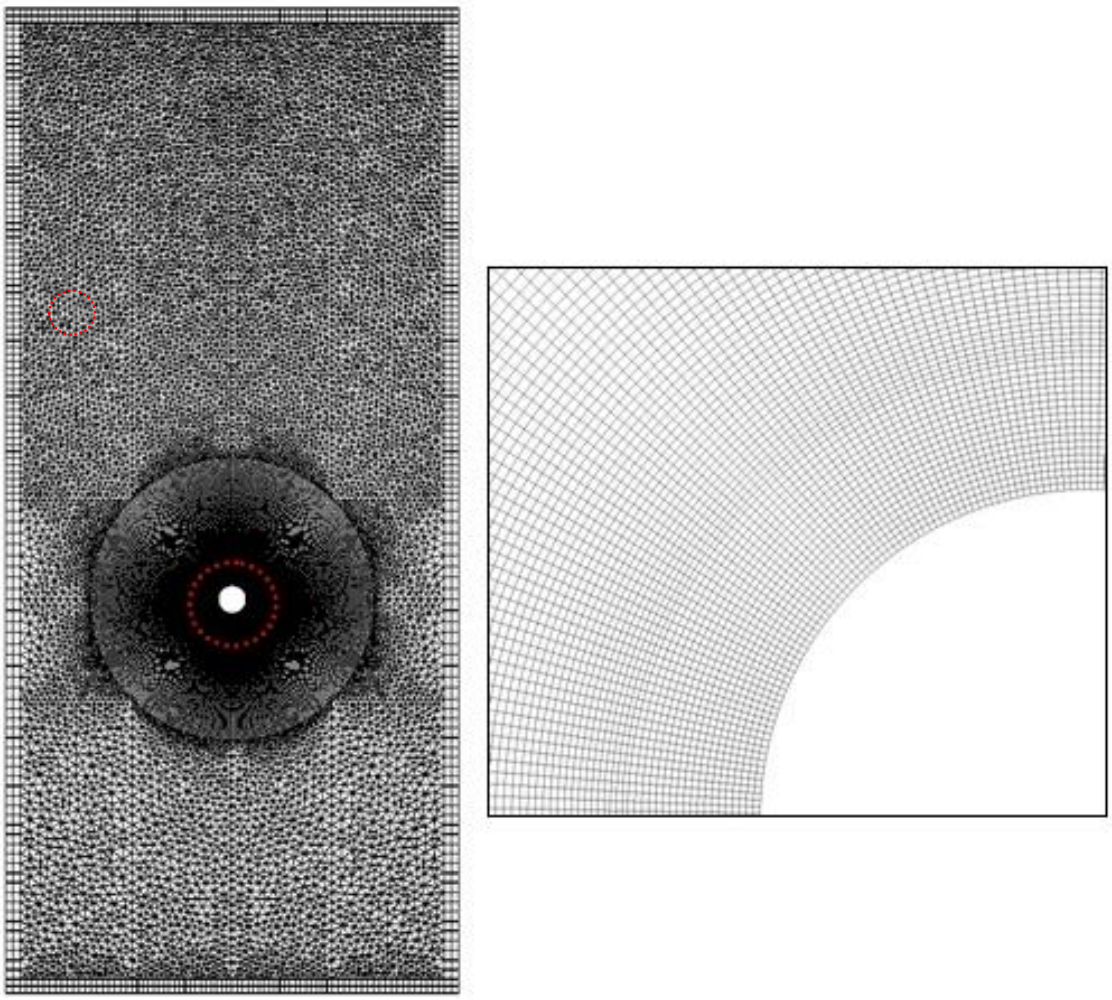

Figure 2 Mesh of the computational domain (left: whole computation space, right: detail of the mesh around the heated cylinder)

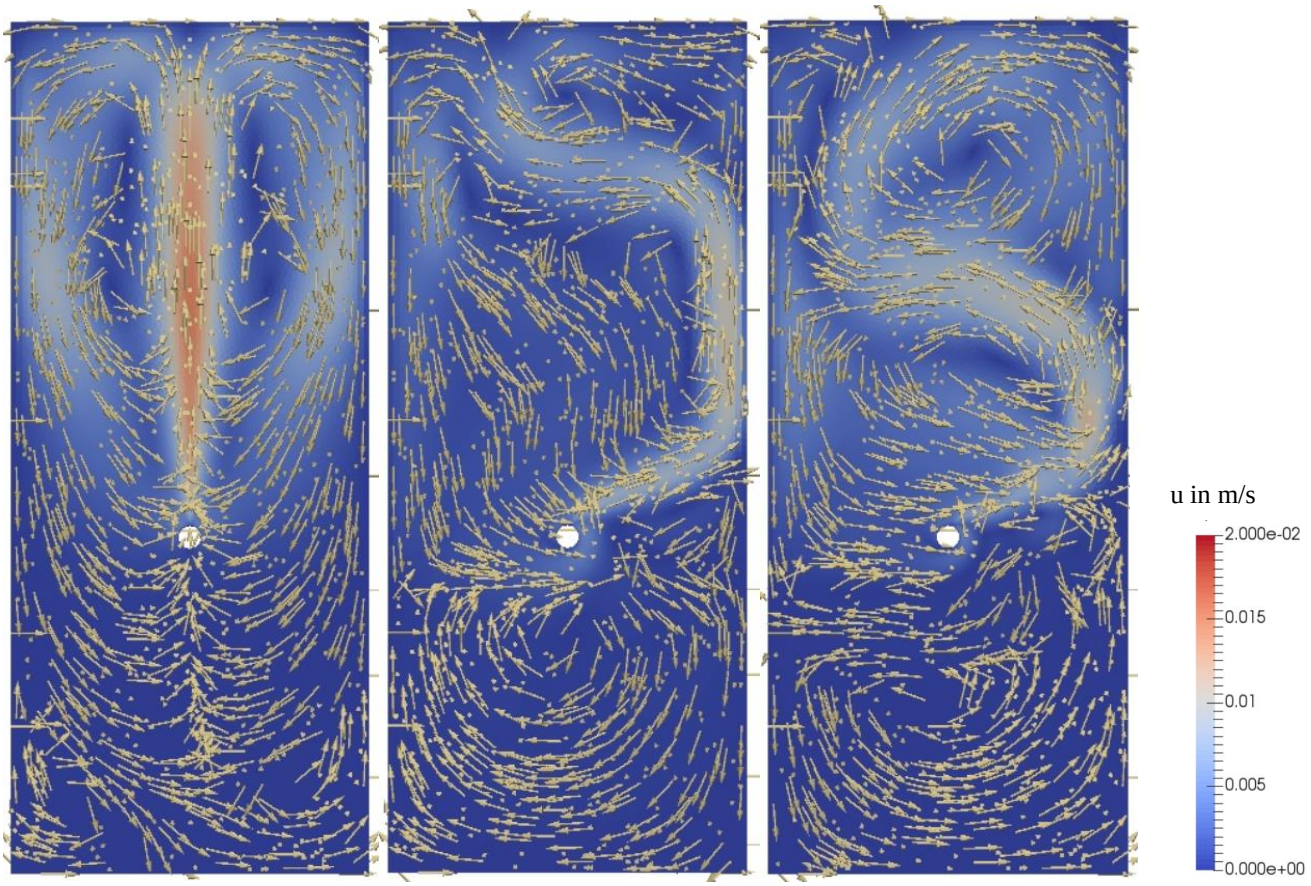

50 s 375 s 800 s

Figure 3 Velocity field (colour: magnitude of velocity, arrows: flow direction) for a heat flux

$$\dot{q} = 10005\,\mathrm{W/m^2}$$

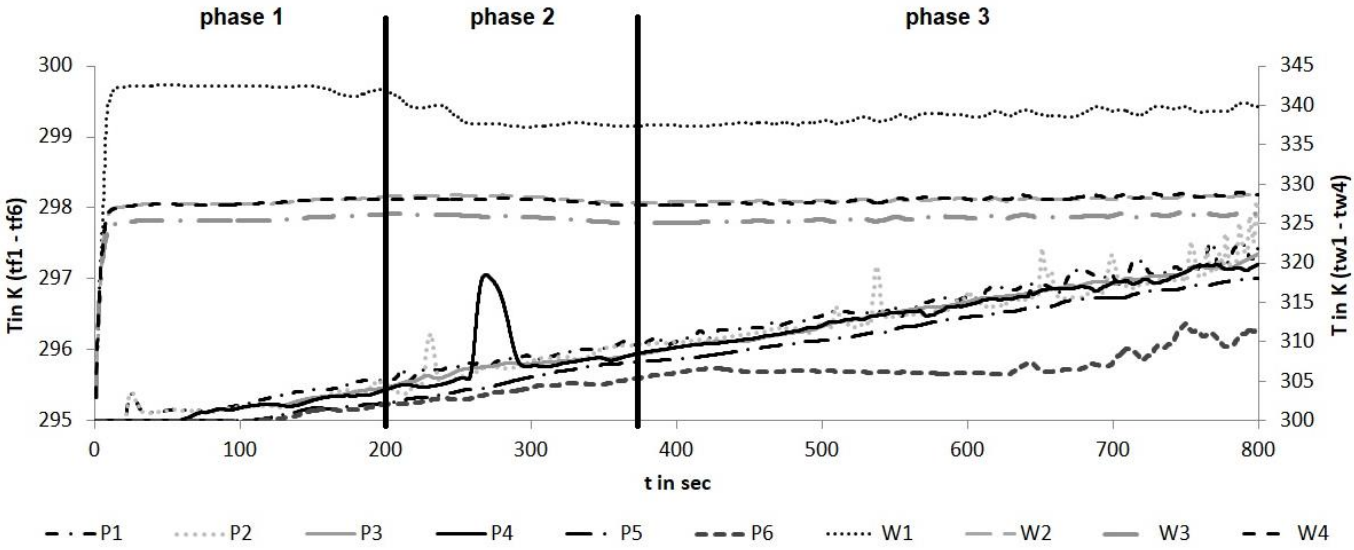

Figure 4 Temperature development with time in diverse locations of the calculation domain

($t_{f1} - t_{f6}$ temperatures in the fluid; $t_{w1} - t_{w4}$ temperatures on the cylinder wall)

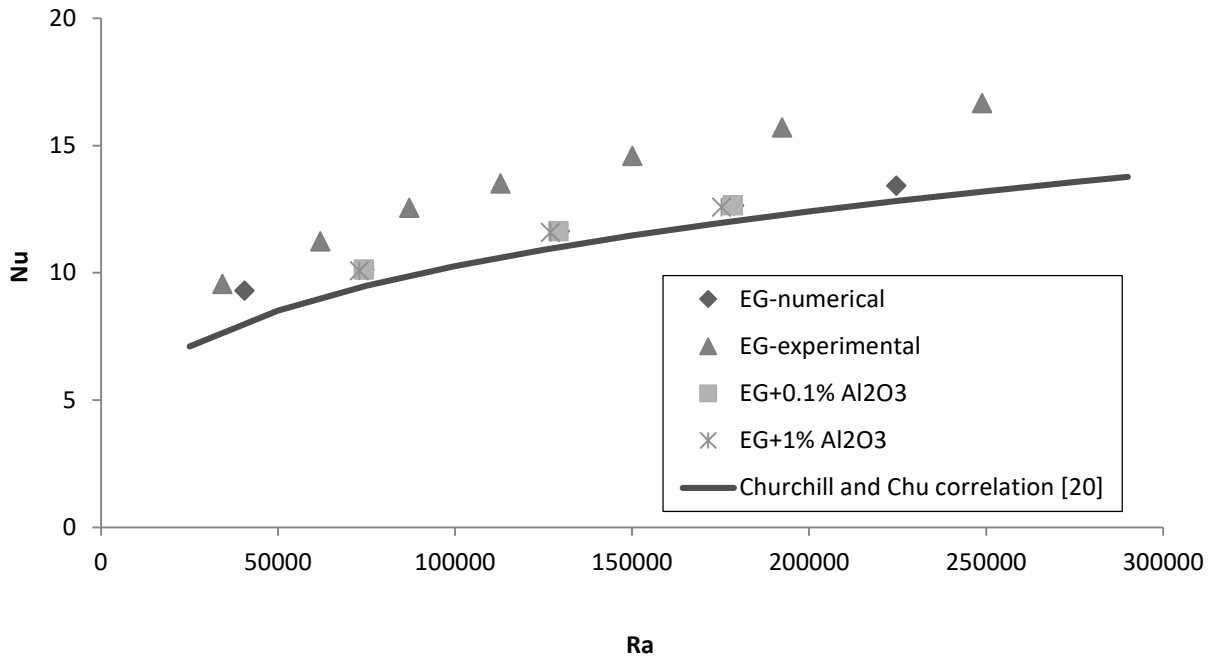

Figure 5 Nusselt versus Rayleigh number from the numerical simulation for EG with and without nanoparticles in comparison to the correlation of Churchill and Chu [20] and preliminary experimental results

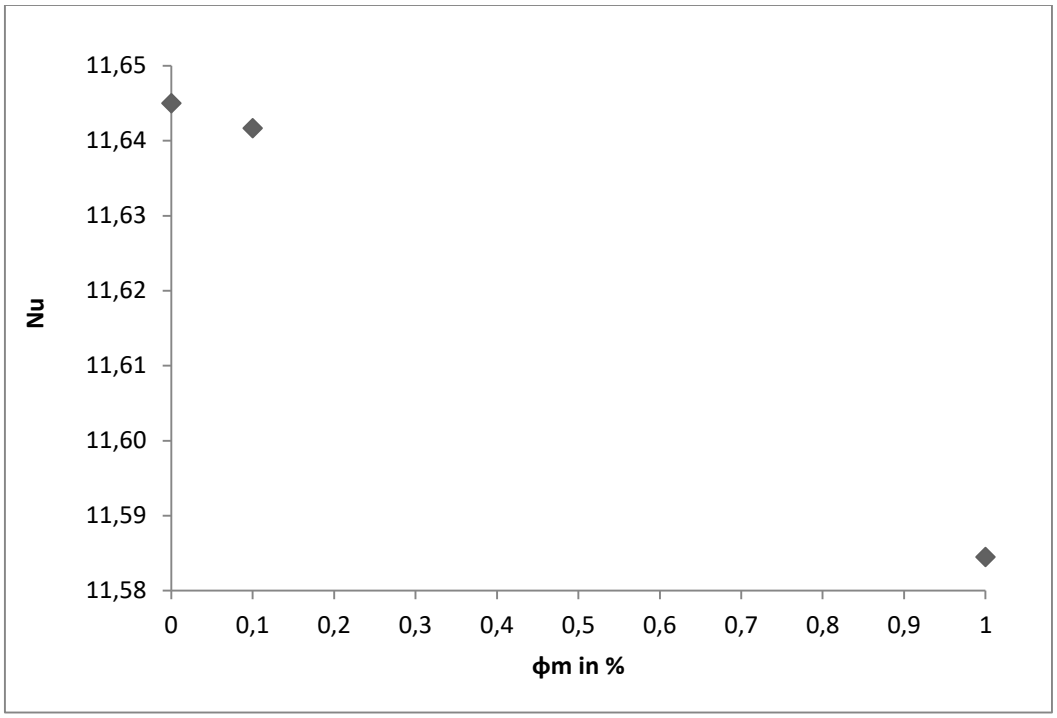

Figure 6 Nusselt number versus nanoparticle concentration for a heat flux $\dot{q} = 10005\, W/m^2$

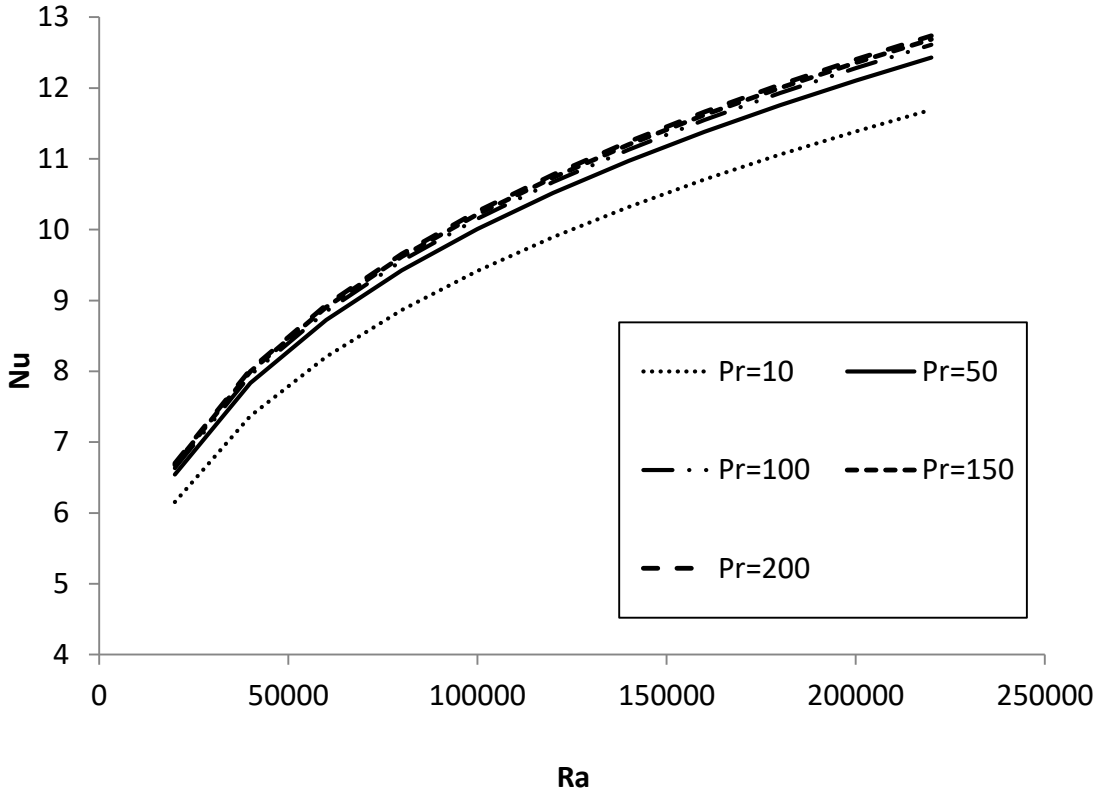

Figure 7 Nusselt versus Rayleigh number for different Prandtl numbers calculated from the correlation of Churchill and Chu [20]

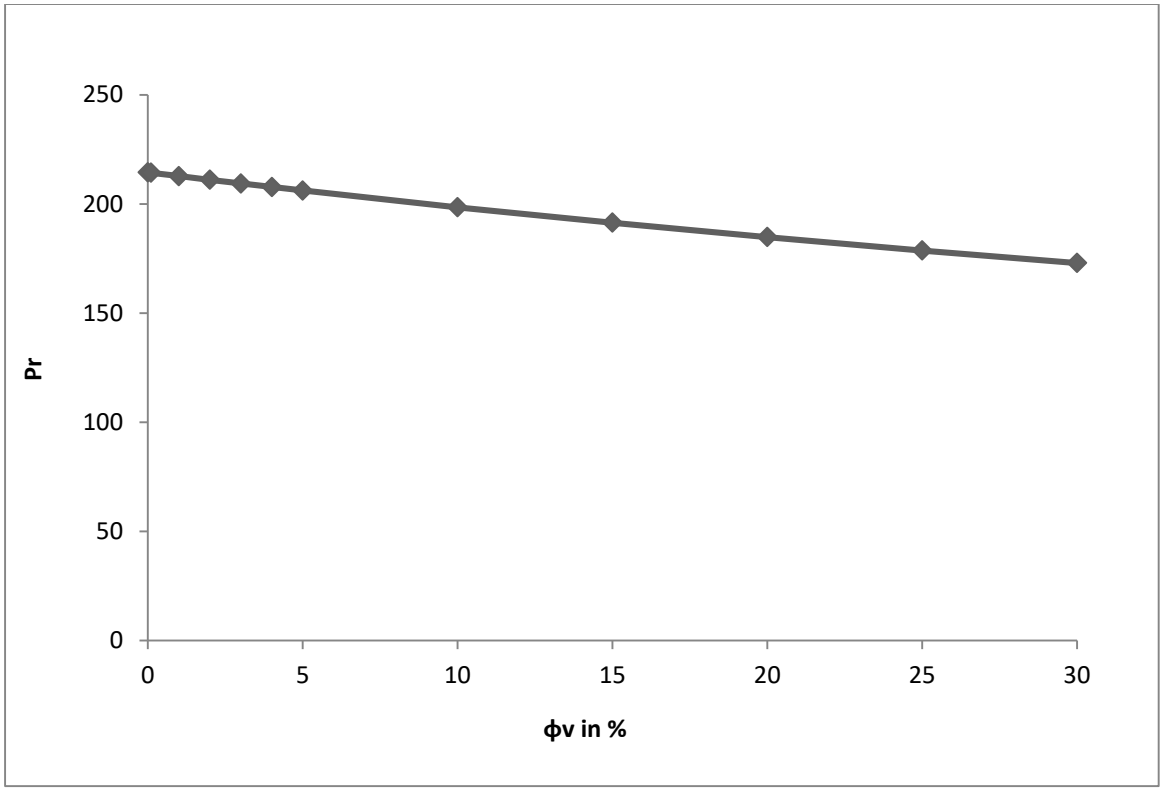

Figure 8 Prandtl number versus concentration of nanoparticles for EG-Al_2O_3 nanofluid and a temperature of 295 K

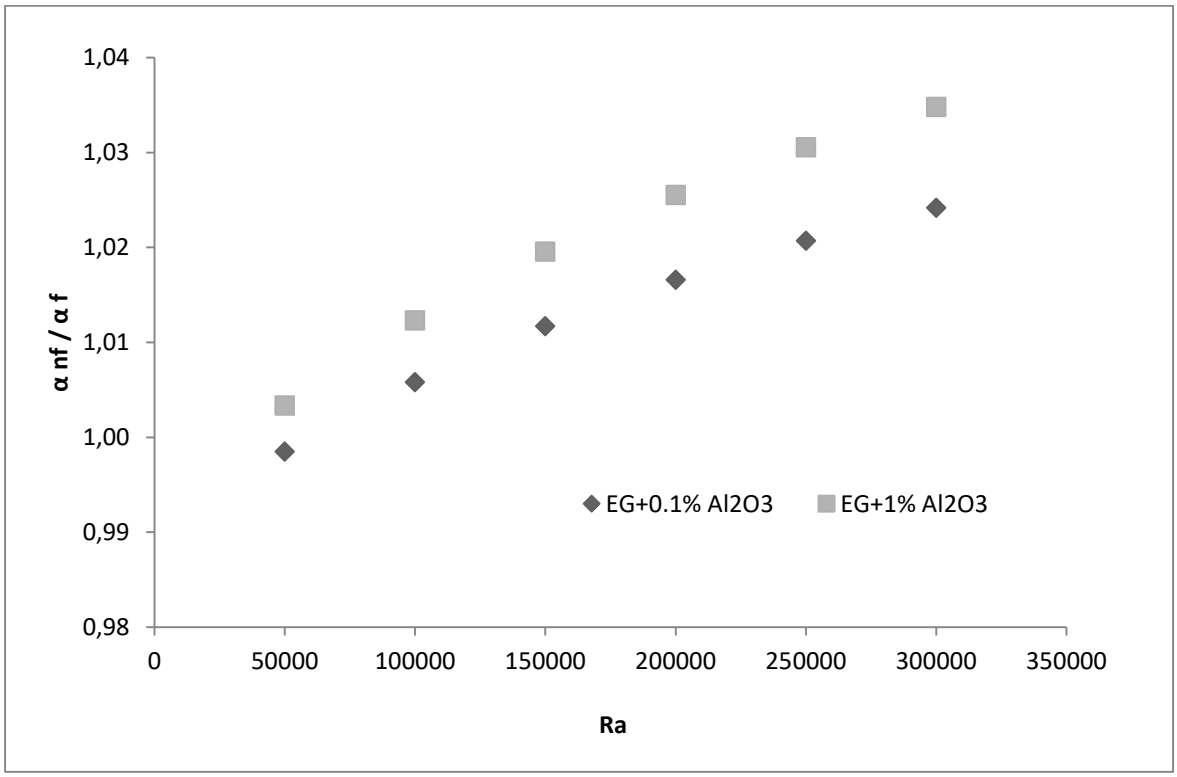

Figure 9 Ratio of heat transfer coefficient with and without nanoparticles versus Rayleigh number for nanoparticle mass concentrations of 0.1% and 1%

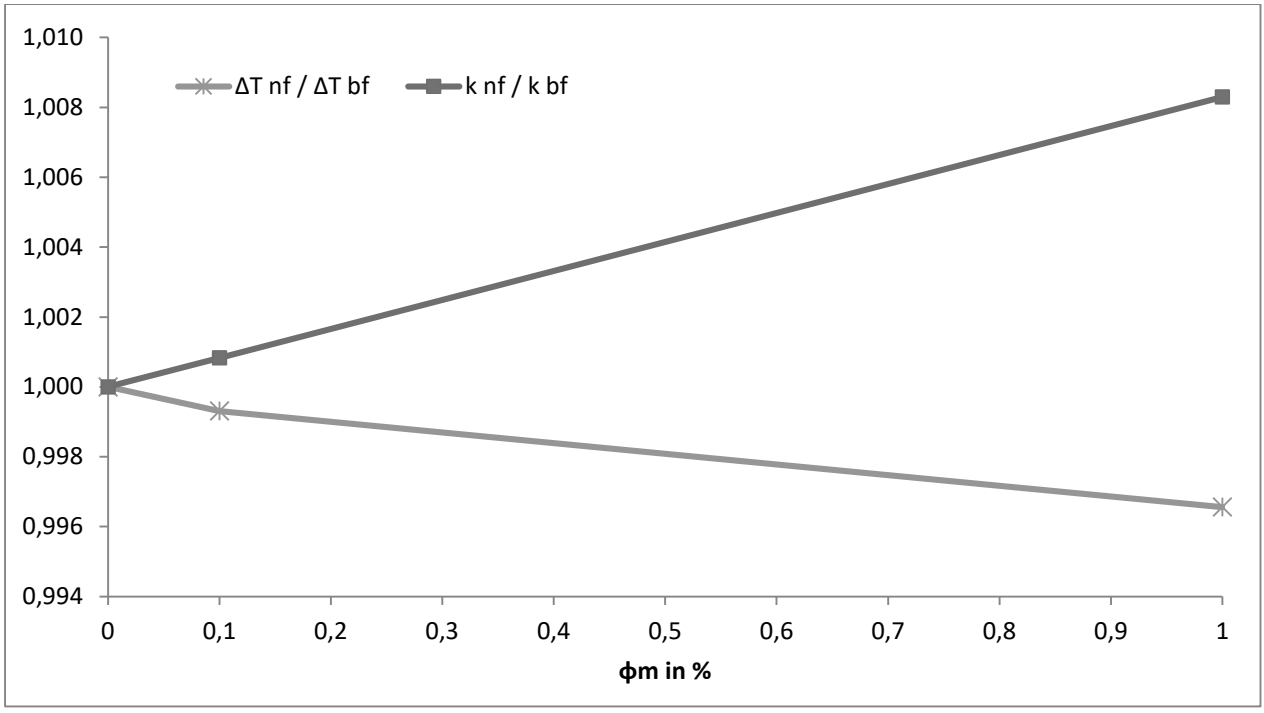

Figure 10 Influence of nanoparticle concentration φ on mean temperature difference between cylinder wall and fluid ΔT as well as heat conductivity k for the heat flux $\dot{q} = 10005\,\mathrm{W/m^2}$.

The plotted quantities for the nanofluid (nf) are related to those of ethylene glycol (bf)

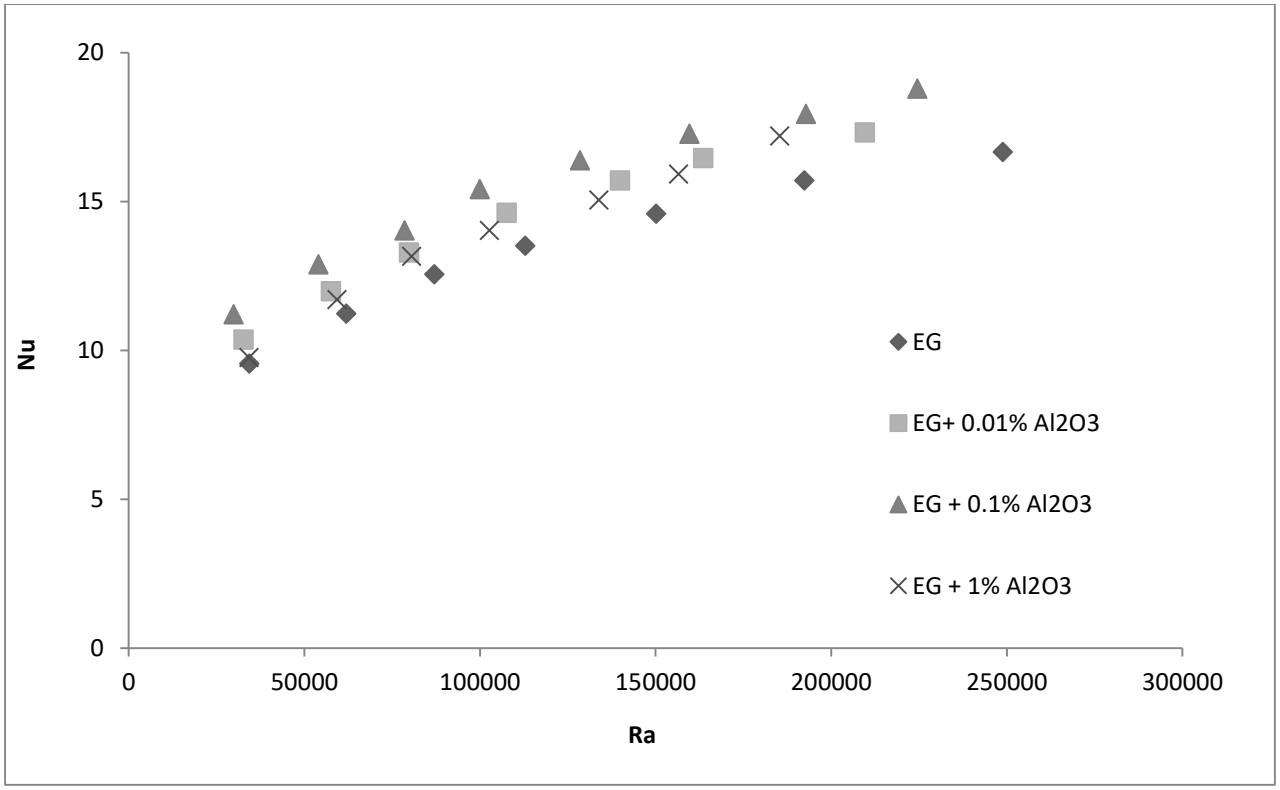

Figure 11 Nusselt versus Rayleigh number for ethylene glycol-Al_2O_3 nanofluids with different nanoparticle mass concentrations from the experimental study

Dorota Sawicka is a PhD candidate. She received her Diploma of Engineer in 2012 and in 2013 a MSc degree in Power Engineering at the Wroclaw University of Technology (Poland). She is currently working on thermophysical properties and free convection heat transfer of nanofluids.

Albert J. Baars is professor of fluid dynamics in the Department of Biomimetics at City University of Applied Sciences Bremen (Germany). He received his diploma in Mechanical Engineering at University of Essen, his PhD at Technical University of Munich and the habilitation at University of Erlangen. His research interests are biological and technical flows using computational fluid dynamics.

Janusz T. Cieśliński received his MSc degree in Mechanical Engineering from Gdansk University of Technology in 1978 as well as his PhD degree in 1986. He also received his DSc degree (habilitation) from Gdansk University of Technology in 1997. In 2002–2008, he served as a vice dean of the Faculty of Mechanical Engineering. In 2006–2010, he was head of the Chair of Ecoengineering and Process Apparatus and in 2010-2017 he was head of the Ecoengineering and Combustion Engines Division. In 2002–2007, he was a chairman of the Multi-Phase Flow and Non-Newtonian Fluids Section of the Polish Academy of Sciences. Since 2011, he is a member of the Committee of Thermodynamics and Combustion of the Polish Academy of Sciences. Since 2008 he is full professor at Gdansk University of Technology, Poland, and since 2016 he is a vice rector of the Gdansk University of Technology.

Sławomir Smoleń is professor and head of Institute for Energy Engineering at City University of Applied Sciences Bremen. He received his MSc degree in Mechanical Engineering from Technical University in Szczecin in 1982 and his PhD degree in 1990/1991. After, he participated in many national and international postdoctoral research projects. In 1996–2000, he worked for Polish and German industrial companies managing projects on the area of energy engineering and energy supply systems. Since 2000, he is professor in Bremen.